International Journal Dental and Medical Sciences Research
Volume 4, Issue 6, Nov-Dec 2022 pp 272-286 www.ijdmsrjournal.com ISSN: 2582-6018

Potential inhibitors of coronavirus 3-chymotrypsin-like protease ($3CL^{pro}$): An in-silico screening of active compounds of Indian Medicinal Plants

Shirshak Singh, Khushal Patel
Ashok & Rita Patel Institute of Integrated Study & Research in Biotechnology and Allied Sciences (ARIBAS) New Vallabh Vidyanagar – 388121

Submitted: 05-11-2022 Accepted: 20-11-2022

ABSTRACT
The novel coronavirus called severe acute respiratory syndrome coronavirus 2 (SARS-CoV-2) and is responsible for the cause of pandemic coronavirus disease 2019 (COVID-19). Main protease ($3CL^{pro}$ or M^{pro}), a cysteine protease that mediates the maturation or cleavage of polyproteins during virus replication and hence could be a promising drug target for combating the coronavirus infection. This study screens some phytoconstituents of Indian medicinal plants that are Withaniasomnifera (Ashwagandha), Ocimum sanctum (Tulsi), and Aloe barbadensis(Aloe Vera) as potential inhibitors of $3CL^{pro}$ using in silico approach. As natural products play a crucial part in repurposing against SARS-CoV-2 infection because it offers minimal and in some cases no toxicity. Molecular docking studies revealed that all selected compounds show significant binding affinities as compared with two reference inhibitors (Lopinavir and Ritonavir) towards SARS-CoV-2 M^{pro}. The top docked compounds were further subjected to scrutinization by Lipinski filtering analysis for drug-likeness or ADMET properties analysis. The ligand-protein interaction study revealed that the selected compounds of Withaniasomnifera: 27-Hydroxywithanone (-7.90 kcal/mol), Physagulin-d (-8.10 kcal/mol), Somniferine (-8.70 kcal/mol), Withanolide A (-8.60 kcal/mol), Withanone (-7.80 kcal/mol), and Withastramonolide (-8.10 kcal/mol) had a binding affinity for ^{Mpro} that surpassed that of the reference inhibitors. Hence, are capable of inhibiting $3CL^{pro}$ with highly conserved inhibitory catalytic dyad residues (CYS^{145} and HIS^{41}) of SARS-CoV-2. The predicted ADME/tox and Lipinski filter analysis suggested that the selected compounds of Withaniasomnifera have an acceptable probability of absorption, distribution, metabolism, excretion, and toxicity. Therefore, these compounds can lead to natural anti-COVID-19 therapeutic agents for combating the pandemic and also be used in both in-vitro, as well as in-vivo models to predict pharmacokinetic properties or to check the preclinical and clinical efficacy for the prevention of COVID-19.

I. INTRODUCTION

The novel coronavirus called severe acute respiratory syndrome coronavirus 2 (SARS-CoV-2), is responsible for the cause of pandemic coronavirus disease 2019 (COVID-19). Normally coronaviruses cause mild upper respiratory tract symptoms and sometimes gastrointestinal infection while highly pathogenic coronavirus like SARS-CoV-2 causes severe flu-like symptoms that tend to acute respiratory distress syndrome (ARDS), pneumonia, renal failure, and death. The incubation period is around 3-6 days. The severity of COVID-19 infection from the onset of infection to death ranges from 6-41 days (varies with age)(Rothan & Byrareddy, 2020).

Common symptoms include cough, cold, sputum production, difficulty breathing, sore throat, muscle pain, headache, fever, chills, fatigue, diarrhea, pneumonia, sometimes multiple ground-glass opacities that led to death (Khalaf et al., 2020).

Coronaviruses are a group of family-related RNA viruses that infects animal and human species and arecomposed of enveloped viruses with positive sense, the single-stranded RNA genome size of 27-32 kb, and a nucleocapsid of helical symmetry (Gyebi et al., 2020). Coronaviruses (family Coronaviridae, subfamily Orthocoronavirinae, order Nidovirales and kingdom Riboviria) are classified into four genera-Alphacoronavirus,Betacoronavirus, Gammacoronavirus, and Deltacoronavirus(Woo et al., 2012). Alphacoronaviruses and betacoronaviruses are originated from bats and infect mammals, whereas gammacoronaviruses and deltacoronaviruses evolved from birds and predominantly infects human species (Wertheim et al., 2013).Among all coronavirus, members are those responsible for the common cold infection, Severe Acute Respiratory Syndrome coronavirus (SARS), Middle East Respiratory

Syndrome-related coronavirus (MERS), and the recently emerged Severe Acute Respiratory Syndrome coronavirus 2 (Eastman et al., 2020).There are six strains of coronaviruses that cause infection to humans that including 229E and NL63 of Alphacoronavirus genus and OC43, HKU1, SARS CoV, and MERS CoV of Betacoronavirus genus (X.-Y. Zhang et al., 2020).Following the spread of SARS CoV-2 led to a global pandemic (officially declared as pandemic on March 11, 2020, by WHO). The novel coronavirus is 88% similar to SARS-CoV and 50% with MERS-CoV. WHO provided data for the reproductive number (R_o) for SARS-CoV-2is 2-2.5 while, for SARS-CoV 1.7-1.9 and MERS with <1, therefore a higher latent of spreading with a high mortality rate of COVID-19 infection is 2.3% which is less than the both of SARS (9.5%) and MERS (34.4%)(Shereen et al., 2020).Currently, there is no proper treatment available that prevents the SARS-CoV-2 infection.Different antiviral drugs and vaccines are used to reduce the severity of symptoms (Chan et al., 2003). Therefore, inhibiting M^{pro} could be a potential drug target by different bioactive compounds which also have potential clinical use.

Table 1: Taxonomic classification and nomenclature of SARS-CoV-2 (Khalaf et al., 2020)

Kingdom	Riboviria
Order	Nidovirales
Family	Coronaviridae
Genus	Betacoronavirus
Subgenus	Sarbecovirus
Species	SARS-relatedcoronavirus
Naming Authority	SARS-CoV-2

M^{pro} as a drug target

M^{pro} plays a vital role in gene expression and replicates processing (by proteolytic cleavage of pp1a and pp1ab into functional polyproteins) (Gyebi et al., 2020). Therefore, viral proteases are most often used as potential drug targets. The inhibitory mechanism of viral protease can reduce the assembly of mature viral particles. To date, many antiviral drugs have been introduced or developed against different viral infections by targeting their proteases. For example, Some FDA approved drugs for Hepatitis C Virus (HCV) NS3/4A protease inhibitors (ritonavir, boceprevir, telaprevir, paritaprevir, asunaprevir, glecaprevir, voxilaprevir, grazoprevir, and sofobuvir) (Leuw & Stephan, 2017) and HIV-1 protease inhibitors (lopinavir, ritonavir, indinavir, tipranavir, darunavir, amprenavir, saquinavir, atazanavir, and nelfinavir) (Wang et al., 2015).

Main protease ($3CL^{pro}$ or M^{pro}), a cysteine protease that mediates the maturation or cleavage of polyproteins during virus replication. It is a homodimer holding twoprotomers each, which consists of three domains (Domain I, II, and III). The residue of Domain I (8–101) and Domain II (102–184), and Domain III (201–303) is linked to domain II by a long loop region (residues 185–200) (Lee et al., 1991).There is a cleft between domains I and II, a Cys-His catalytic dyad site which is also known as a substrate-binding site. Cys-His catalytic dyad plays a vital role in proteolytic activity. The Cys-His catalytic dyad site is comprised of four subsites namely; S1', S1, S2, and S4. The main protease is a conserved protein among all coronaviruses and the amino acids in substrates are identified as - from N-terminus to the C-terminus - P4-P3-P2-P1 and P1'-P2'-P3'(Yang et al., 2003). The M^{pro} also known as nsp5, encoded by ORF1ab, that cleaves two important overlapping polyproteins (pp1a and pp1ab) into 16 non-structural proteins(nsp1-16) which plays an important role in viral replication and maturation. These important roles of the viral protease enzyme drive itself as a noteworthy therapeutic target for restricting coronavirus-related diseases (L. Zhang et al., 2020).

Two FDA (The Food and Drug Administration) approved antiviral drugs are - **Lopinavir** and **Ritonavir**. Both have the property of inhibiting protease protein of HIV (Human Immunodeficiency Virus). Therefore both drugs were used as **referenceinhibitors** to study on main protease protein of SARS-CoV2. (Chandwani & Shuter, 2008; Chan et al., 2003; Das et al., 2021).Screening

phytoconstituents of medicinal plants possessing antiviral activity or having properties to boost immune system and identification of its target (M^{pro}) relics one of the most important norms for the discovery of new molecules as well as to assess the therapeutic efficacy of existing drug/bioactive molecules(Cherrak et al., 2020).Therefore, in this study bioactive compounds of three Indian medicinal plants were used: Withaniasomnifera, Ocimum sanctum,and Aloe barbadensis.Ashwagandha (Withaniasomnifera), a Rasayana (rejuvenator) has the property to enhance the physical as well as mental state, which rejuvenates the body's weakness and improves longevity. And it also has anti-inflammatory, anti-microbial, anti-diabetic, anti-tumor, anti-stress, neuroprotective, cardioprotective, and immunomodulatory effects. Active ingredients contain Withanoside I-VII and Somniferine contains many biological actions (Shree et al., 2020).Tulsi (Ocimum sanctum), also known as "Mother Medicine of Nature" and has medicinal and spiritual properties. It is also known as the sanctified herb. It has many therapeutic properties (mainly leaves are used) comprises of anti-viral, immunomodulatory, adaptogenic, antimicrobial, anti-inflammatory, cardioprotective, anti-fungal, anti-bacterial, anti-diabetic, anti-cancer, analgesic, anti-fertility, and hepatoprotective action. The main phytoconstituents of tulsi are Vicenin and Ursolic acid which have many biological applications (Cohen, 2014).Aloe vera (Aloe barbadensis), is one of the eldest and widely used medicinal plants. The phenolic compounds, flavonoids, and alkaloids have a broad range of pharmacological activity such as anti-inflammatory, anti-microbial, anti-diabetic, anti-tumour. Some of the bioactive compounds that are isolated from the leaf extract of Aloe vera are Aloin, Umbelliferone, Aloe-emodin, and Vanillic acid that have many biological actions (Majumder et al., 2020).

Investigation of new chemical phytoconstituents of several plants and its pharmacological screening will help in developing a new life-saving drug. The stems, roots, seeds, and leaves of medicinal plants contain a variety of phytoconstituents that have many biological activities including flavonoids, alkaloids, saponins, phenolic compounds, stilbenes, tannins, terpenoids, etc(Das et al., 2021;Ghosh et al., 2021; Lin et al., 2017;Pandit & Singh, 2020;Giofrè et al., 2021)

II. MATERIALS AND METHODS

Protein Preparation

Retrieval of the crystal structure of M^{pro} was done using RCSB Protein Data Bank (https://www.rcsb.org/) (PDB ID - 6LU7) in 'PDB' Format(Shree et al., 2020). Target protein preparation was done using AutoDock4(Morris et al., 2009). Existing ligand (N3 inhibitor), hetatom, and water molecules were removed. Usually, crystal structures of proteins lack hydrogen atoms so the addition of polar hydrogen and charge were used to provide electrostatics during docking, Grid setup was done and prepared protein was saved in 'pdbqt'format for molecular docking.

Ligand Preparation

Retrieval of the 3D structure of selected ligand molecules and reference inhibitors (Lopinavir and Ritonavir) in SDF (Structural Data Format) format was done using PubChem database (https://pubchem.ncbi.nlm.nih.gov/) and these downloaded SDF format converted to PDB format using OPEN BABEL software(O'Boyle et al., 2011). Preparation of ligand molecules was done similar to protein using AutoDock Tool and was saved in 'pdbqt'format(S. Kim et al., 2021).

Molecular Docking

Molecular docking was done between selected ligand molecules or reference inhibitorswith M^{pro} of SARS-CoV-2 using AutoDock Vina(Trott & Olson, 2010). The binding affinities obtained were recorded and analyzed. Virtual screening was done using Discovery Studio Visualizer to ensure the interacted residues of $M^{pro}$with respective ligands (Gyebi et al., 2020).

Analysis of drug properties

Drug properties of respective ligand molecules were analyzed using drug-likeness and ADME/tox prediction.The 3D-SDF files were downloaded or canonical SMILES were copied from the PubChem database for further evaluation of drug properties. For drug-likeness, Lipinski's Rule of Five (**Ro5**) (http://www.scfbio-iitd.res.in/) was used(Lipinski, 2004;Benet et al., 2016; Tallei et al., 2020). For ADMET (Absorption, Distribution, Metabolism, Excretion, and Toxicity) prediction, ADMETlab 2.0 web-based tool was used (https://admetmesh.scbdd.com/).

III. RESULTS AND DISCUSSION

Molecular Docking

Molecular docking study revealed that different bioactive molecules Aloe barbadensis (Aloe vera), Ocimum sanctum (Tulsi), and Withaniasomnifera (Ashwagandha), shows significant binding affinities towards SARS-CoV-2 M^{pro}. The results of binding

International Journal Dental and Medical Sciences Research
Volume 4, Issue 6, Nov-Dec 2022 pp 272-286 www.ijdmsrjournal.com ISSN: 2582-6018

affinities were used to screen out best-docked ligand molecules reference to Lopinavir and Ritonavir at rmsd – 0. The binding affinity of **Lopinavir** and **Ritonavir** for M^{pro} was **-7.3** and **-7.3** Kcal.mol^{-1}, respectively. The top docked bioactive compounds with docking scores that surpassed that of reference inhibitors suggest their promising efficacy and potential inhibitors of SARS-CoV-2(Gyebi et al., 2020). The active compounds with more negative values of docking score have more binding affinities that interacted more strongly than other phytoconstituents to M^{pro}.

It was observed that all selected compounds of Withaniasomnifera had a binding affinity for M^{pro} that surpassed that of the reference inhibitors. Therefore, the top 2 docked bioactive compounds are

Table 2: Screened Ligand molecules with their binding affinities

S No.	Compound Name	Plant Source	Chemical formula	PubChem CID	Binding affinities(Kcal.mol^{-1})
1	**Lopinavir**	-	$C_{37}H_{48}N_4O_5$	92727	**-7.30**
2	**Ritonavir**	-	$C_{37}H_{48}N_6O_5S_2$	392622	**-7.30**
3	Aloe Emodin	Aloe barbadensis	$C_{15}H_{10}O_5$	10207	-7.00
4	Aloenin		$C_{19}H_{22}O_{10}$	162305	-7.60
5	Aloesin		$C_{19}H_{22}O_9$	160190	-8.00
6	Altechromone A		$C_{11}H_{10}O_3$	5316891	-6.20
7	Barbaloin		$C_{21}H_{22}O_9$	12305761	-8.00
8	Chrysophanol		$C_{15}H_{10}O_4$	10208	-7.00
9	Saikochromone A		$C_{11}H_{10}O_5$	10013795	-6.00
10	Umbelliferone		$C_9H_6O_3$	5281426	-5.60
11	Vanillic acid		$C_8H_8O_4$	8468	-5.10
12	10-Hydroxyaloin B		$C_{21}H_{22}O_{10}$	14889737	-7.60
13	Apigenin	Ocimum sanctum	$C_{15}H_{10}O_5$	5280443	-7.70
14	Carvacrol		$C_{10}H_{14}O$	10364	-4.80
15	beta-Caryophyllene		$C_{15}H_{24}$	5281515	-5.10
16	Cirsimaritin		$C_{17}H_{14}O_6$	188323	-7.30
17	Estragole		$C_{10}H_{12}O$	8815	-4.50
18	Eugenol		$C_{10}H_{12}O_2$	3314	-5.00
19	Isothymusin		$C_{17}H_{14}O_7$	630253	-7.20
20	Linalool		$C_{10}H_{18}O$	6549	-4.30
21	Rosmarinic acid		$C_{18}H_{16}O_8$	5281792	-6.90
22	Ursolic acid		$C_{30}H_{48}O_3$	64945	-7.60

International Journal Dental and Medical Sciences Research
Volume 4, Issue 6, Nov-Dec 2022 pp 272-286 www.ijdmsrjournal.com ISSN: 2582-6018

23	27-Hydroxywithanone	Withaniasomnifera	$C_{28}H_{38}O_7$	21574483	-7.90
24	Physagulin-d		$C_{34}H_{52}O_{10}$	10100412	-8.10
25	**Somniferine**		$C_{36}H_{36}N_2O_7$	14106343	**-8.70**
26	**Withanolide A**		$C_{28}H_{38}O_6$	11294368	**-8.60**
27	Withanone		$C_{28}H_{38}O_6$	21679027	-7.80
28	Withastramonolide		$C_{28}H_{38}O_7$	21607602	-8.10

Note: Compounds having binding affinities > 7.3 (Green), or binding affinities <7.3 (Red)

Somniferine (**-8.7** Kcal.mol^{-1}) and **Withanolide A(-8.6** Kcal.mol^{-1}), while, only two compounds fromOcimum sanctum showed slightly higher than reference inhibitors that are **Apigenin** (**-7.7** Kcal.mol^{-1}) and **Ursolic acid(-7.6** Kcal.mol^{-1}). whereas, four compounds from Aloe barbadensis have higher binding affinities than reference inhibitors that are **Aloenin** (**-7.6** Kcal.mol^{-1}), **10-Hydroxyaloin B** (**-7.6** Kcal.mol^{-1}), **Aloesin** (**-8.0** Kcal.mol^{-1}), and **Barbaloin** (**-8.0** Kcal.mol^{-1}). (**Table 3.1)**. Both top docked compounds were found to be the highest binding affinities than other screened compounds which means, they interacted more strongly than other phytoconstituents to M^{pro} of SARS-CoV-2.

Some of the phytoconstituents from Ayurvedic medicinal plants Withaniasomnifera (Ashwagandha), Tinospora cordifolia (Giloy), and Ocimum sanctum (Tulsi) have shown promising effects against SARS-CoV-2 targets. Study reports of phytochemicals namely Withanoside V, Somniferine, Tinocordiside, Vicenin, Isorientin 40-O-glucoside 200-O-p-hydroxybenzoate, and Ursolic acid obtained from medicinal plants, have predicted significant binding energy as compared to the native ligand N3, so they can play a vital role in the inhibition of M^{pro} of SARS-CoV-2. The binding of these recognized bioactive phytoconstituents with SARS-CoV-2 M^{pro} decreases the progression of viral transcription and replication by down turning the cleavage of polyproteins that release viral non-structural proteins(Shree et al., 2020).The target protein was further subjected to docked with N3 inhibitor using AutoDock vina.The docking score was found to be significant(**-6.6** Kcal.mol^{-1}), as compared to the reference inhibitors.Therefore,selected phytoconstituents can exhibit similar binding interactions(Gyebi et al., 2020).

Table 3: Interacting amino acid residues of M^{pro} of SARS-CoV-2 with top docked compounds

Compound Name	**Interacted Residues**	**Interacted Residues involved in H-Bonding**
Lopinavir	THR^{26}, GLU^{166}, GLN^{189}, MET^{165}, HIS^{41}, MET^{49}	THR^{26}, GLU^{166}, GLN^{189}, MET^{165}
Ritonavir	GLU^{166}, LEU^{167}, PRO^{168}, HIS^{41}, MET^{49}, MET^{165}, GLN^{189}, HIS164	GLU^{166,} GLN^{189}, HIS^{164}
Withanolide A	CYS^{145}, MET^{165}	CYS^{145}
Somniferine	ASN^{142}, SER^{46}, GLU^{166}, CYS^{145}, MET^{165}	ASN^{142}, SER^{46}, GLU^{166}

International Journal Dental and Medical Sciences Research
Volume 4, Issue 6, Nov-Dec 2022 pp 272-286 www.ijdmsrjournal.com ISSN: 2582-6018

Amino acid interaction of selected bioactive compounds with M^{pro}

The interaction of reference inhibitors and top-ranked bioactive compounds with the amino acid of M^{pro} of SARS-CoV-2 are represented in Table 3

The outcome of the ligand-protein binding interaction showed that reference inhibitors were docked into receptor binding sites and catalytic dyad (CYS^{145} and HIS^{41}) of the SARS-CoV-2**.** Lopinavir interacted via conventional hydrogen bond with THR^{26}, GLU^{166}, and GLN^{189}; carbon-hydrogen bond to MET^{165}; Pi cation to HIS^{41} and Pi-Sulfur bond with MET^{49}(**Table 3**)(**Figure 1**).Ritonavir interacted via conventional hydrogen bond with GLU^{166}; Amide-Pi stacking with LEU^{167}; Pi-Sigma with PRO^{168}; Pi-Cation to HIS^{41}; Pi alkyl with MET^{49}, MET-165 and carbon-hydrogen bond with GLN^{189} and HIS^{164}(**Table** 3)(**Figure** 2). Both of the reference inhibitors interacted with catalytic-dyad (CYS^{145} and HIS^{41}) with only Pi-Cation interaction. Interaction of compounds with ASN^{142} and

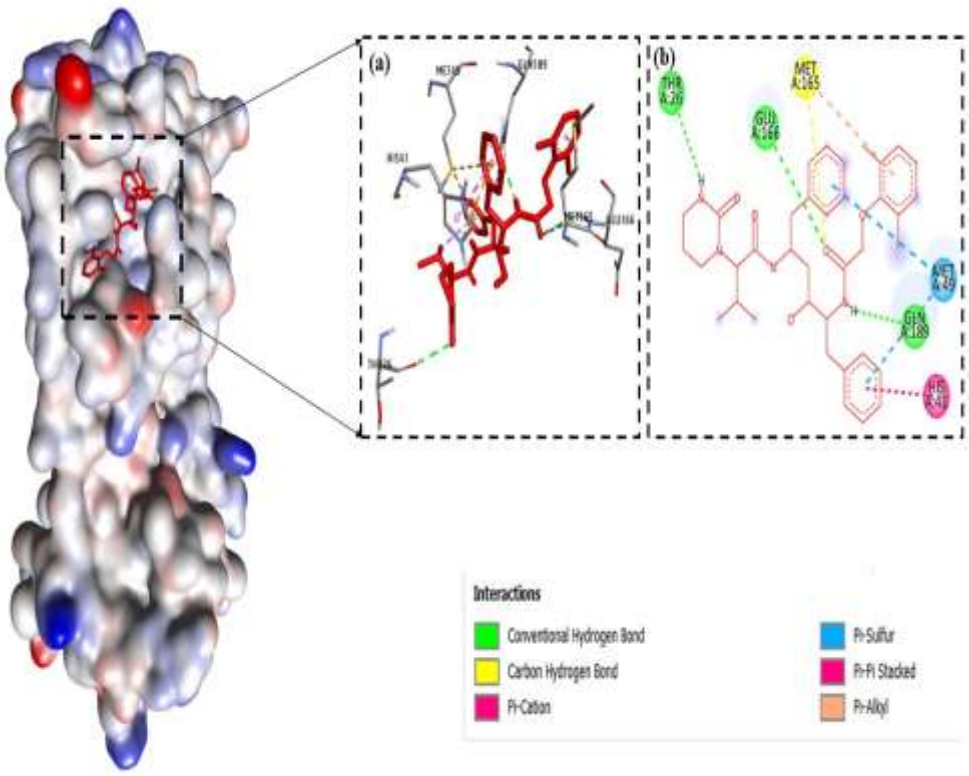

Figure 1: Visualization of SARS-CoV-2 ^{Mpro} amino acid interaction with Lopinavir (a) 3D interaction view with important residue (b) 2D interaction view

International Journal Dental and Medical Sciences Research
Volume 4, Issue 6, Nov-Dec 2022 pp 272-286 www.ijdmsrjournal.com ISSN: 2582-6018

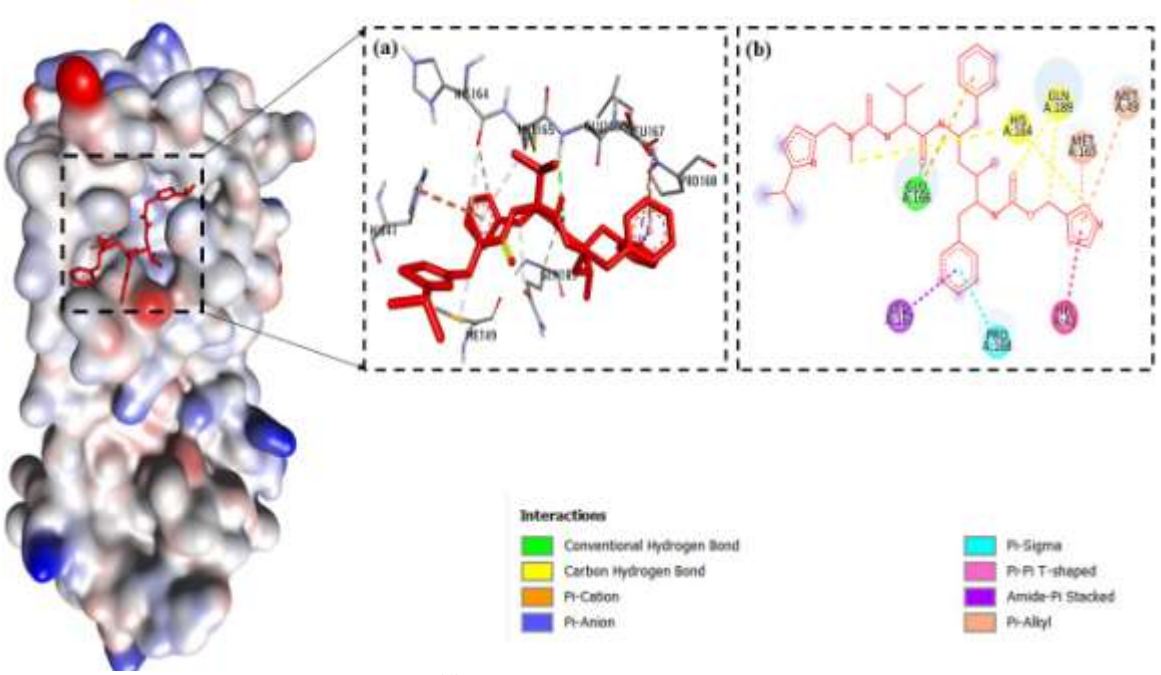

Figure 2: Visualization of SARS-CoV-2 M^{pro} amino acid interaction with Ritonavir (a) 3D interaction view with important residue (b) 2D interaction view

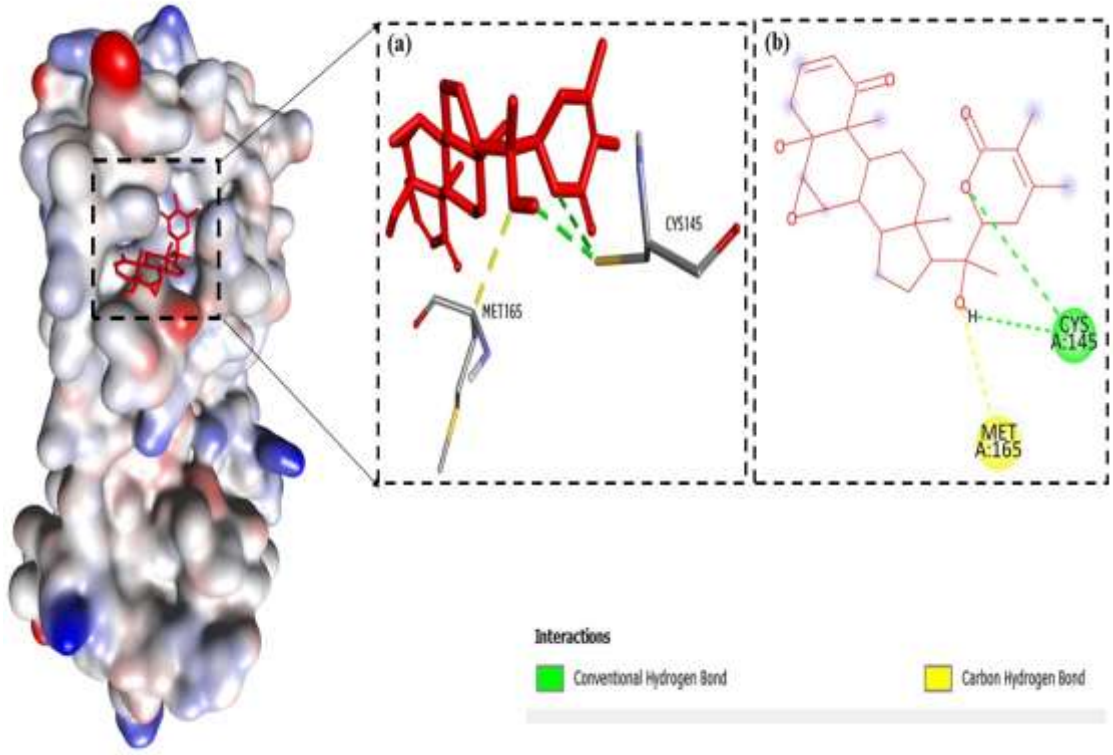

Figure 3: Visualization of SARS-CoV-2 M^{pro} amino acid interaction with Withanolide A (a) 3D interaction view with important residue (b) 2D interaction view

International Journal Dental and Medical Sciences Research
Volume 4, Issue 6, Nov-Dec 2022 pp 272-286 www.ijdmsrjournal.com ISSN: 2582-6018

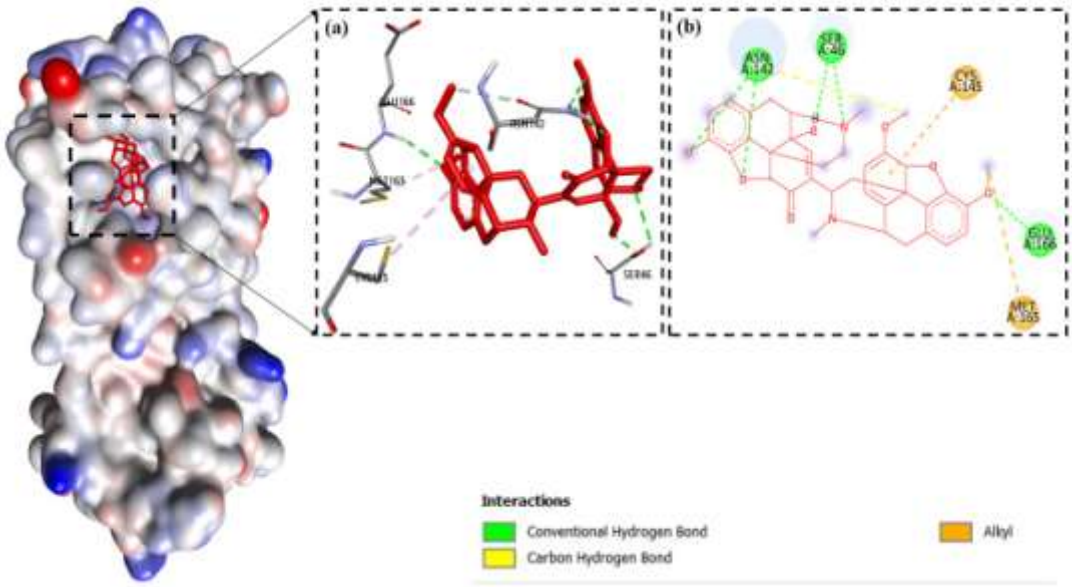

Figure 4: Visualization of SARS-CoV-2 M^{pro}amino acid interaction with Somniferine (a) 3D interaction view with important residue (b) 2D interaction view

ASP^{187}can augment the catalytic activity of M^{pro}(Zhao et al., 2008).Somniferine, the topmost docked compound to the $M^{pro}$of SARS-CoV-2 interacted via conventional hydrogen bond with ASN^{142}, SER^{46}, and GLU^{166}; and Alkyl interaction with catalytic-dyad (CYS^{145} and HIS^{41}) and MET^{165}(**Table** 3)(**Figure** 4).While, Withanolide A, the second most docked compound to the $M^{pro}$of SARS-CoV-2 interacted via conventional hydrogen bond with catalytic-dyad (CYS^{145} and HIS^{41}) and carbon-hydrogen bond with MET^{165}(**Table** 3)(**Figure** 3). Similar research was done in which the selected phytoconstituents of medicinal plants were docked into the conserved region that is catalytic-dyad (CYS^{145} and HIS^{41}) of M^{pro}, and interacting amino acid residues with ligands were MET^{49}, ASN^{142}, THR^{24}, THR^{25}, THR^{26}, GLU^{166}, GLN^{189}, GLY^{143}, HIS^{164}, CYS^{44}, THR^{45},and SER^{46} (Qamar et al., 2020).

The ligand-protein interaction of Withanolide A to SARS-CoV-2 that targeted the Cys-His catalytic-dyad (CYS^{145} and HIS^{41})) with conventional hydrogen bond but Somniferine with alkyl interaction along with the other interactions with different binding residues, the docking of bioactive compounds revealed that the SARS-CoV-2 interacted with the same ligand differently. Similar research on Withanoside V showed significant binding interaction with catalytic-dyad with having binding energy (-10.32 $Kcal.mol^{-1}$)(Shree et al., 2020), these compounds were found in roots of W. somniferatestified as tachyphylaxis inhibition activity(Matsuda et al., 2001).A similar ligand-binding outline unveiled by ritonavir, cryptoquindoline, 10-hydroxyusambarensine, 6-oxoisoiguesterin, and 20-Epi-isoiguesterinol to the catalytic-dyad designates the inhibition of M^{pro}(Gyebi et al., 2020).

The result revealed from this study that all compounds were docked into the Cys-His catalytic-dyad (CYS^{145} and HIS^{41}) of the coronaviruses M^{pro} in a similar pattern as reference inhibitors (Lopinavir and Ritonavir) but Somniferine and withanolide A are the top compounds amongst all others. The binding pattern of selected compounds was found to be in the conserved region of catalytic-dyad that makes it more beneficial against anti-viral activities of SARS-CoV-2. The concluding amino acid residues are supposed to provide the opportunity for the substrate in the active site of the M^{pro} of SARS-CoV and SARS-CoV-2. (Yang et al., 2003). However, catalytic-dyad could be a promising target for inhibitors because of its perilous importance in the role of viral protease enzyme (Anand et al., 2003).

IV. DRUG PROPERTIES

The results obtained from Lipinski filtering analysis and ADMET study are shown in**Table 4.**

International Journal Dental and Medical Sciences Research
Volume 4, Issue 6, Nov-Dec 2022 pp 272-286 www.ijdmsrjournal.com ISSN: 2582-6018

Drug Likeness

Lipinski's Rule of Five (**Ro5**)distinguishes between drug-like and non-drug-like molecules. The drug-likeness evaluates the chances of drug molecules to become an oral drug concerning bioavailability. **Ro5** states that an orally bioactive drug should not have more than one violation of the four criteria were used Drug Likeness study for the best-docked compounds: Molecular Mass (<500 Dalton), High Lipophilicity (cLogP<5), Hydrogen Bond Donor (<5), and Hydrogen Bond Acceptor (<10) (Lipinski, 2004).The Lipinski rule suggests that if a compound shows more than one violation, then it shows low solubility, poor absorption, and permeation(Benet et al., 2016; Tallei et al., 2020).

Almost all compounds meet Ro5 criteria except **Physagulin-D** having higher binding affinities but violate the Ro5 with Molecular mass greater than 500 Dalton (**620.80 Dalton**) and more than 5 Hydrogen Bond Donor (**6**)**(Table 4).** However, compounds that violate only one Ro5 criterion are **Barbaloin** (**7**) and **10-Hydroxyaloin** B (**8**) with more than 5 Hydrogen Bond Donor, **Somniferine** (**608.70Dalton**)with Molecular mass greater than 500 Dalton, and **Ursolic acid** (7.09) with cLogP greater than 5. This indicates that all bioactive compounds except Physagulin-D are competent to be used as drug-like molecules.cLogP values of **Aloesin** (-0.35), **Barbaloin** (-0.89), and **10-Hydroxyaloin B** (-1.79) are found to be less than zero and therefore considered as favorable for drug-likeness.cLogP values less than zero are considered favorable for drug-likeness of a given compound as it is correlated to water solubility and hence contributes to bioavailability (Elipilla, 2015).

ADMET Study

From scrutinization by ADMET properties of bioactive compounds suggested that all selected compounds from Withaniasomnifera(27-Hydroxywithanone, Physagulin-d, Somniferine, Withanolide A, Withanone, and Withastramonolide)shows a high probability of absorption, distribution, metabolism, and excretion (**Table 5)**. Hence, poor bioavailability may cause a novel drug to fail clinical trials, even if it has high efficacy in prior in vitro or in vivo assessments (M.T.Kim et al., 2014). These selected compounds are found to be non-toxic, non-carcinogenic, and bind specifically to the catalytic binding sites of M^{pro}.

Table 4: Lipinski's Rule of Five of selected bioactive compounds

Compound Name	Properties				Violations	Meet Ro5 Criteria
	Molecular Mass (Da)	Hydrogen Bond Donor	Hydrogen Bond Acceptor	cLogP		
Aloe Emodin	**270.24**	**3**	**5**	**1.37**	**0**	**Yes**
Aloenin	**410.40**	**5**	**10**	**0.69**	**0**	**Yes**
Aloesin	**394.40**	**5**	**9**	**-0.35**	**0**	**Yes**
Altechromone A	**190.19**	**1**	**3**	**2.18**	**0**	**Yes**
Barbaloin	**418.40**	**7**	**9**	**-0.89**	**1**	**Yes**
Chrysophanol	**254.24**	**2**	**4**	**2.18**	**0**	**Yes**
Saikochromone A	**222.19**	**2**	**5**	**0.85**	**0**	**Yes**
Umbelliferone	**162.14**	**1**	**3**	**1.32**	**0**	**Yes**
Vanillic acid	**168.15**	**2**	**4**	**1.10**	**0**	**Yes**
10-Hydroxyaloin B	**434.40**	**8**	**10**	**-1.79**	**1**	**Yes**

International Journal Dental and Medical Sciences Research
Volume 4, Issue 6, Nov-Dec 2022 pp 272-286 www.ijdmsrjournal.com ISSN: 2582-6018

Apigenin	**270.24**	**3**	**5**	**2.42**	**0**	**Yes**
Carvacrol	**150.22**	**1**	**1**	**2.82**	**0**	**Yes**
beta-Caryophyllene	**204.35**	**0**	**0**	**4.73**	**0**	**Yes**
Cirsimaritin	**314.29**	**2**	**6**	**2.73**	**0**	**Yes**
Estragole	**148.20**	**0**	**1**	**2.42**	**0**	**Yes**
Eugenol	**164.20**	**1**	**2**	**2.13**	**0**	**Yes**
Isothymusin	**330.29**	**3**	**7**	**2.44**	**0**	**Yes**
Linalool	**154.25**	**1**	**1**	**2.67**	**0**	**Yes**
Rosmarinic acid	**360.30**	**5**	**8**	**1.76**	**0**	**Yes**
Ursolic acid	**456.70**	**2**	**3**	**7.09**	**1**	**Yes**
27-Hydroxywithanone	**486.60**	**3**	**7**	**2.47**	**0**	**Yes**
Physagulin-d	**620.80**	**6**	**10**	**1.98**	**2**	**No**
Somniferine	**608.70**	**2**	**9**	**2.71**	**1**	**Yes**
Withanolide A	**470.60**	**2**	**6**	**3.50**	**0**	**Yes**
Withanone	**470.60**	**2**	**6**	**3.50**	**0**	**Yes**
Withastramonolide	**486.60**	**3**	**7**	**2.32**	**0**	**Yes**

Note: Green - Meet Ro5 criteria, while, Red – Violates Ro5 criteria

Table 5: Physicochemical properties of selected bioactive compounds

Compounds	**Absorption**					**Distribution**			**Metabolism**		**Excretion**		**Toxicity**		
									CYP1A2						
	HIA	Caco-2 Permeability	P-gp substrate	P-gp inhibitor	$F_{20\%}$	Plasma Protein Binding	V_d	BBB Penetration	Substrate	Inhibitors	Clearance	$T_{1/2}$	AMES Toxicity	Acute Oral Rat Toxicity	Carcinogenicity
Aloe Emodin	0.91	1.04	0.00	0.00	0.81	0.97	0.45	0.01	0.13	0.96	4.87	0.82	0.59	0.02	0.11
Aloenin	0.87	1.13	0.98	0.00	0.26	0.70	0.84	0.56	0.22	0.06	5.47	0.49	0.12	0.04	0.04
Aloesin	0.84	1.11	1.00	0.00	0.07	0.74	0.99	0.32	0.10	0.02	1.75	0.51	0.71	0.44	0.02
Altechromone A	0.01	0.95	1.00	0.00	0.72	0.86	0.83	0.04	0.94	0.98	7.38	0.76	0.44	0.06	0.11
Barbaloin	1.00	1.18	0.01	0.00	0.83	0.92	1.13	0.07	0.04	0.06	2.33	0.50	0.72	0.05	0.04

Chrysophanol	0.01	0.99	0.00	0.03	0.06	1.00	0.46	0.14	0.41	0.95	6.21	0.14	0.89	0.23	0.91
Saikochromone A	0.09	0.98	0.96	0.00	0.12	0.75	0.95	0.04	0.90	0.96	7.62	0.86	0.56	0.04	0.03
Umbelliferone	0.01	0.94	0.99	0.00	0.99	0.86	0.60	0.08	0.85	0.97	13.58	0.83	0.05	0.38	0.84
Vanillic acid	0.01	1.03	0.00	0.00	0.01	0.53	0.36	0.44	0.69	0.04	7.90	0.94	0.02	0.05	0.06
10-Hydroxyaloin B	0.97	1.20	0.10	0.00	0.98	0.70	1.37	0.40	0.04	0.03	1.39	0.25	0.68	0.14	0.05
Apigenin	0.02	0.97	0.82	0.00	1.00	0.97	0.51	0.01	0.15	0.99	7.02	0.86	0.48	0.06	0.28
Carvacrol	0.01	0.89	0.01	0.01	0.93	0.93	2.57	0.83	0.95	0.94	11.34	0.67	0.03	0.22	0.27
beta-Caryophyllene	0.00	0.90	0.00	0.42	0.89	0.95	4.14	0.83	0.52	0.37	9.94	0.05	0.01	0.05	0.36
Cirsimaritin	0.02	0.95	0.40	0.58	0.01	0.94	0.68	0.01	0.96	0.92	4.61	0.78	0.43	0.07	0.19
Estragole	0.00	0.86	0.00	0.00	0.06	0.91	1.05	0.66	0.95	0.97	12.05	0.58	0.14	0.03	0.74
Eugenol	0.01	0.87	0.00	0.00	0.73	0.92	0.83	0.19	0.94	0.90	14.04	0.89	0.07	0.12	0.81
Isothymusin	0.04	0.98	0.00	0.97	0.01	0.93	0.68	0.00	0.94	0.85	3.40	0.83	0.48	0.22	0.21
Linalool	0.00	0.88	0.00	0.02	0.13	0.85	1.51	0.95	0.28	0.16	9.74	0.49	0.01	0.02	0.24
Rosmarinic acid	0.23	1.20	0.00	0.00	0.51	0.98	0.37	0.05	0.04	0.14	15.35	0.96	0.04	0.45	0.28
Ursolic acid	0.01	1.04	0.00	0.00	0.01	0.99	0.82	0.72	0.43	0.01	3.67	0.02	0.01	0.18	0.03
27-Hydroxywithanone	0.32	0.98	0.08	0.03	0.01	0.69	0.67	1.00	0.27	0.01	9.83	0.09	0.02	0.96	0.20
Physagulin-d	0.88	1.05	0.03	0.02	0.03	0.88	0.85	0.06	0.09	0.00	2.58	0.09	0.06	0.33	0.14
Somniferine	0.01	1.06	0.03	1.00	0.98	0.73	1.78	0.93	0.52	0.01	9.06	0.05	0.10	1.00	0.83
Withanolide A	0.08	0.95	0.01	0.98	0.02	0.86	1.62	1.00	0.48	0.01	16.29	0.07	0.02	0.93	0.14
Withanone	0.13	0.97	0.01	0.59	0.01	0.84	1.35	1.00	0.40	0.01	16.44	0.05	0.02	0.96	0.34
Withastramonolide	0.51	0.97	0.52	0.01	0.01	0.28	0.61	0.97	0.15	0.01	12.83	0.11	0.01	0.87	0.09

Note: Green-Excellent, Yellow- Moderate, and Red- Poor

In contrast to this, except Physagulin-d almost all compounds show Rat Oral Acute Toxicity parameters. An effective drug should achieve the body's homeostasis of biochemical behavior, pharmacokinetics (ADMET), and safety. This profile is critical for the success of novel drug discovery. Most precisely an ideal drug should be taken in the appropriate amount into the body, distributed rationally to various organs and tissues, metabolized in such a way that does not instantly eradicate its activity, eliminated appropriately, and established non-toxicity. (Xiong et al., 2021). The interactions of drug molecules with cytochrome P450 isoforms are of two types: enzyme induction (as substrate) or enzyme inhibition (as inhibitors). Enzyme inhibition reduces the metabolism, but induction can increase the metabolism of drug molecules. (Bibi, 2008)

In-silico techniques have been introduced for the development and discovery of drugs as a tool that predicts drug's ADMETox properties at the early stages (Boobiset al., 2002).

The development of new methods and technologies in the prediction of drugs ADMET properties has taken drug development maneuvers to an advanced level, in-silico prediction techniques were shown to be functional along with in vivo as well as in vitro tests to facilitate drug discovery and development approaches (Moroyet al., 2012).

V. CONCLUSION

In conclusion, this study revealed that that natural phytoconstituents from Aloe barbadensis, Ocimum sanctum, and Withaniasomnifera plants are capable of inhibiting $3CL^{pro}$ or M^{pro} with highly conserved inhibitory catalytic dyad residues (CYS^{145} and HIS^{41}) of SARS-CoV-2.

From molecular docking studies and scrutinization by Lipinski rule or ADMET properties suggested that all selected compounds from Withaniasomnifera(27-Hydroxywithanone, Physagulin-d, Somniferine, Withanolide A, Withanone, and Withastramonolide)shows significant binding affinities towards SARS-CoV-2 M^{pro} and also have an acceptable probability of absorption, distribution, metabolism, excretion, and toxicity. Therefore, these compounds can be used in both in-vitro, as well as in-vivo models to predict pharmacokinetic properties or to check the preclinical and clinical efficacy for the prevention of COVID-19.

Acknowledgment
The authors are grateful to ARIBAS and Charutar Vidya Mandal for providing a Bioinformatics facility during this study.
Funding
This study was not funded.

REFERENCES

[1]. Anand, K., Ziebuhr, J., Wadhwani, P., Mesters, J. R., & Hilgenfeld, R. (2003). Coronavirus main proteinase (3CLpro) Structure: Basis for design of anti-SARS drugs. Science, 300(5626), 1763–1767. https://doi.org/10.1126/science.1085658

[2]. Benet, L. Z., Hosey, C. M., Ursu, O., & Oprea, T. I. (2016). BDDCS, the Rule of 5 and Drugability Leslie. Advanced Drug Delivery Reviews, 101(1), 89–98. https://doi.org/10.1016/j.addr.2016.05.007.BDDCS

[3]. Bibi, Z. (2008). Role of cytochrome P450 in drug interactions. Nutrition & Metabolism, 5(1), 27. https://doi.org/10.1186/1743-7075-5-27

[4]. Chan, K. S., Lai, S. T., Chu, C. M., Tsui, E., Tam, C. Y., Wong, M. M. L., Tse, M. W., Que, T. L., Peiris, J. S. M., Sung, J., Wong, V. C. W., & Yuen, K. Y. (2003). Treatment of severe acute respiratory syndrome with lopinavir/ritonavir: A multicentre retrospective matched cohort study. Hong Kong Medical Journal, 9(6), 399–406.

[5]. Cherrak, S. A., Merzouk, H., & Mokhtari-Soulimane, N. (2020). Potential bioactive glycosylated flavonoids as SARS-CoV-2 main protease inhibitors: A molecular docking and simulation studies. PLOS ONE, 15(10), e0240653. https://doi.org/10.1371/journal.pone.0240653

[6]. Cohen, M. (2014). Tulsi - Ocimum sanctum: A herb for all reasons. Journal of Ayurveda and Integrative Medicine, 5(4), 251. https://doi.org/10.4103/0975-9476.146554

[7]. Das, A., Pandita, D., Jain, G. K., Agarwal, P., Grewal, A. S., Khar, R. K., & Lather, V. (2021). Role of phytoconstituents in the management of COVID-19. In Chemico-Biological Interactions (Vol. 341, Issue 1, p. 109449). https://doi.org/10.1016/j.cbi.2021.109449

[8]. Eastman, R. T., Roth, J. S., Brimacombe, K.

R., Simeonov, A., Shen, M., Patnaik, S., & Hall, M. D. (2020). Remdesivir: A Review of Its Discovery and Development Leading to Emergency Use Authorization for Treatment of COVID-19. ACS Central Science, 6(5), 672–683. https://doi.org/10.1021/acscentsci.0c00489

[9]. Elipilla, P. (2015). Designing, molecular docking, and toxicity studies of novel plasmepsin II inhibitors. European Journal of Biotechnology and Bioscience ~, 27(9), 27–30.

[10]. Ghosh, R., Chakraborty, A., Biswas, A., & Chowdhuri, S. (2021). Identification of alkaloids from Justicia adhatoda as potent SARS CoV-2 main protease inhibitors: An in silico perspective. Journal of Molecular Structure, 1229, 129489. https://doi.org/10.1016/j.molstruc.2020.129489

[11]. Giofrè, S. V., Napoli, E., Iraci, N., Speciale, A., Cimino, F., Muscarà, C., Molonia, M. S., Ruberto, G., & Saija, A. (2021). Interaction of selected terpenoids with two SARS-CoV-2 key therapeutic targets: An in silico study through molecular docking and dynamics simulations. Computers in Biology and Medicine, 134(May), 104538. https://doi.org/10.1016/j.compbiomed.2021.104538

[12]. Gyebi, G. A., Ogunro, O. B., Adegunloye, A. P., Ogunyemi, O. M., & Afolabi, S. O. (2020). Potential inhibitors of coronavirus 3-chymotrypsin-like protease (3CL pro): an in silico screening of alkaloids and terpenoids from African medicinal plants. Journal of Biomolecular Structure and Dynamics, 39(9), 1–13. https://doi.org/10.1080/07391102.2020.1764868

[13]. Khalaf, K., Papp, N., Chou, J. T.-T., Hana, D., Mackiewicz, A., & Kaczmarek, M. (2020). SARS-CoV-2: Pathogenesis, and Advancements in Diagnostics and Treatment. Frontiers in Immunology, 11(10), 570927. https://doi.org/10.3389/fimmu.2020.570927

[14]. Kim, M. T., Sedykh, A., Chakravarti, S. K., Saiakhov, R. D., & Zhu, H. (2014). Critical Evaluation of Human Oral Bioavailability for Pharmaceutical Drugs by Using Various Cheminformatics Approaches. Pharmaceutical Research, 31(4), 1002–1014. https://doi.org/10.1007/s11095-013-1222-1

[15]. Kim, S., Chen, J., Cheng, T., Gindulyte, A., He, J., He, S., Li, Q., Shoemaker, B. A., Thiessen, P. A., Yu, B., Zaslavsky, L., Zhang, J., & Bolton, E. E. (2021). PubChem in 2021: new data content and improved web interfaces. Nucleic Acids Research, 49(D1), D1388–D1395. https://doi.org/10.1093/nar/gkaa971

[16]. Lee, H.-J., Shieh, C.-K., Gorbalenya, A. E., Koonin, E. V., La Monica, N., Tuler, J., Bagdzhadzhyan, A., & Lai, M. M. C. (1991). The complete sequence (22 kilobases) of murine coronavirus gene 1 encoding the putative proteases and RNA polymerase. Virology, 180(2), 567–582. https://doi.org/10.1016/0042-6822(91)90071-I

[17]. Leuw, P. de, & Stephan, C. (2017). Protease inhibitors for the treatment of hepatitis C virus infection 2013 improved SVR rates, the amount of severe side effects was high. GMS Infectious Diseases, 5, 1–14. https://doi.org/10.3205/id000034

[18]. Lin, S.-C., Ho, C.-T., Chuo, W.-H., Li, S., Wang, T. T., & Lin, C.-C. (2017). Effective inhibition of MERS-CoV infection by resveratrol. BMC Infectious Diseases, 17(1), 144. https://doi.org/10.1186/s12879-017-2253-8

[19]. Lipinski, C. A. (2004). Lead- and drug-like compounds: the rule-of-five revolution. Drug Discovery Today: Technologies, 1(4), 337–341. https://doi.org/10.1016/j.ddtec.2004.11.007

[20]. Majumder, R., Parida, P., Paul, S., & Basak, P. (2020). In vitro and in silico study of Aloe vera leaf extract against human breast cancer. Natural Product Research, 34(16), 2363–2366. https://doi.org/10.1080/14786419.2018.1534848

[21]. Matsuda, H., Murakami, T., Kishi, A., & Yoshikawa, M. (2001). Structures of withanosides I, II, III, IV, V, VI, and VII, new withanolide glycosides, from the roots of Indian Withania somnifera DUNAL. and inhibitory activity for tachyphylaxis to clonidine in isolated guinea-pig ileum. Bioorganic and Medicinal Chemistry, 9(6), 1499–1507. https://doi.org/10.1016/S0968-0896(01)00024-4

[22]. Morris, G. M., Huey, R., Lindstrom, W., Sanner, M. F., Belew, R. K., Goodsell, D. S., & Olson, A. J. (2009). AutoDock4 and AutoDockTools4: Automated docking with selective receptor flexibility. Journal of

Computational Chemistry, 30(16), 2785–2791. https://doi.org/10.1002/jcc.21256

[23]. O'Boyle, N. M., Banck, M., James, C. A., Morley, C., Vandermeersch, T., & Hutchison, G. R. (2011). Open Babel. Journal of Cheminformatics, 3(33), 1–14. https://jcheminf.biomedcentral.com/track/pdf/10.1186/1758-2946-3-33

[24]. Pandit, R. D., & Singh, R. K. (2020). COVID-19 Ayurveda treatment protocol of governments of Nepal and India: a review and perspective. Applied Science and Technology Annals, 1(1), 72–80. https://doi.org/10.3126/asta.v1i1.30276

[25]. Qamar, T. ul, Muhammad, Alqahtani, S. M., Alamri, M. A., & Chen, L. L. (2020). Structural basis of SARS-CoV-2 3CLpro and anti-COVID-19 drug discovery from medicinal plants. Journal of Pharmaceutical Analysis, 10(4), 313–319. https://doi.org/10.1016/j.jpha.2020.03.009

[26]. Rothan, H. A., & Byrareddy, S. N. (2020). The epidemiology and pathogenesis of coronavirus disease (COVID-19) outbreak. Journal of Autoimmunity, 109(February), 102433. https://doi.org/10.1016/j.jaut.2020.102433

[27]. Shereen, M. A., Khan, S., Kazmi, A., Bashir, N., & Siddique, R. (2020). COVID-19 infection: Emergence, transmission, and characteristics of human coronaviruses. Journal of Advanced Research, 24, 91–98. https://doi.org/10.1016/j.jare.2020.03.005

[28]. Shree, P., Mishra, P., Selvaraj, C., Singh, S. K., Chaube, R., Garg, N., & Tripathi, Y. B. (2020). Targeting COVID-19 (SARS-CoV-2) main protease through active phytochemicals of ayurvedic medicinal plants – Withania somnifera (Ashwagandha), Tinospora cordifolia (Giloy) and Ocimum sanctum (Tulsi) – a molecular docking study. Journal of Biomolecular Structure and Dynamics, 0(0), 1–14. https://doi.org/10.1080/07391102.2020.1810778

[29]. Shuter, J. (2008). Lopinavir/ritonavir in the treatment of HIV-1 infection: a review. Therapeutics and Clinical Risk Management, Volume 4(5), 1023–1033. https://doi.org/10.2147/TCRM.S3285

[30]. Tallei, T. E., Tumilaar, S. G., Niode, N. J., Fatimawali, Kepel, B. J., Idroes, R., Effendi, Y., Sakib, S. A., & Emran, T. Bin. (2020). Potential of Plant Bioactive Compounds as SARS-CoV-2 Main Protease (Mpro) and Spike (S) Glycoprotein Inhibitors: A Molecular Docking Study. Scientifica, 2020, 1–18. https://doi.org/10.1155/2020/6307457

[31]. Trott, O., & Olson, A. J. (2010). AutoDock Vina: Improving the speed and accuracy of docking with a new scoring function, efficient optimization, and multithreading. Journal of Computational Chemistry, 31(1), 455–461. https://doi.org/10.1002/jcc.21334

[32]. Wang, Y., Lv, Z., & Chu, Y. (2015). HIV protease inhibitors: a review of molecular selectivity and toxicity. HIV/AIDS - Research and Palliative Care, 7, 95. https://doi.org/10.2147/HIV.S79956

[33]. Wertheim, J. O., Chu, D. K. W., Peiris, J. S. M., Kosakovsky Pond, S. L., & Poon, L. L. M. (2013). A Case for the Ancient Origin of Coronaviruses. Journal of Virology, 87(12), 7039–7045. https://doi.org/10.1128/JVI.03273-12

[34]. Woo, P. C. Y., Lau, S. K. P., Lam, C. S. F., Lau, C. C. Y., Tsang, A. K. L., Lau, J. H. N., Bai, R., Teng, J. L. L., Tsang, C. C. C., Wang, M., Zheng, B.-J., Chan, K.-H., & Yuen, K.-Y. (2012). Discovery of Seven Novel Mammalian and Avian Coronaviruses in the Genus Deltacoronavirus Supports Bat Coronaviruses as the Gene Source of Alphacoronavirus and Betacoronavirus and Avian Coronaviruses as the Gene Source of Gammacoronavirus and Deltacoronavi. Journal of Virology, 86(7), 3995–4008. https://doi.org/10.1128/JVI.06540-11

[35]. Xiong, G., Wu, Z., Yi, J., Fu, L., Yang, Z., Hsieh, C., Yin, M., Zeng, X., Wu, C., Lu, A., Chen, X., Hou, T., & Cao, D. (2021). ADMETlab 2.0: an integrated online platform for accurate and comprehensive predictions of ADMET properties. Nucleic Acids Research, 49(1), 5–14. https://doi.org/10.1093/nar/gkab255

[36]. Yang, H., Yang, M., Ding, Y., Liu, Y., Lou, Z., Zhou, Z., Sun, L., Mo, L., Ye, S., Pang, H., Gao, G. F., Anand, K., Bartlam, M., Hilgenfeld, R., & Rao, Z. (2003). The crystal structures of severe acute respiratory syndrome virus main protease and its complex with an inhibitor. Proceedings of the National Academy of Sciences, 100(23), 13190–13195. https://doi.org/10.1073/pnas.1835675100

[37]. Zhang, L., Lin, D., Sun, X., Curth, U., Drosten, C., Sauerhering, L., Becker, S., Rox, K., & Hilgenfeld, R. (2020). Crystal structure of SARS-CoV-2 main protease provides a basis for design of improved α-ketoamide inhibitors. Science, 368(6489), 409–412. https://doi.org/10.1126/science.abb3405

[38]. Zhang, X.-Y., Huang, H.-J., Zhuang, D.-L., Nasser, M. I., Yang, M.-H., Zhu, P., & Zhao, M.-Y. (2020). Biological, clinical and epidemiological features of COVID-19, SARS and MERS and AutoDock simulation of ACE2. Infectious Diseases of Poverty, 9(1), 99. https://doi.org/10.1186/s40249-020-00691-6

[39]. Zhao, Q., Li, S., Xue, F., Zou, Y., Chen, C., Bartlam, M., & Rao, Z. (2008). Structure of the Main Protease from a Global Infectious Human Coronavirus, HCoV-HKU1. Journal of Virology, 82(17), 8647–8655. https://doi.org/10.1128/jvi.00298-08